Communications Research Centre

THE STRUCTURE OF HCl DOPED SILICON OXIDES AND OF THE OVERLAYING METALLIZATION

by

M. BOUCHARD, W.A. HARTMAN AND R.M. KULEY

TK
5102.5
C673e
#1298

IC Department of Communications Ministère des Communications

CRC REPORT NO. 1298

OTTAWA, OCTOBER 1976

DATE OF DISPLAY

JAN 25 1977

COMMUNICATIONS RESEARCH CENTRE

DEPARTMENT OF COMMUNICATIONS
CANADA

THE STRUCTURE OF HCl DOPED SILICON OXIDES AND OF THE OVERLAYING METALLIZATION

by

M. Bouchard, W.A. Hartman and R.M. Kuley

(Space Technology Branch)

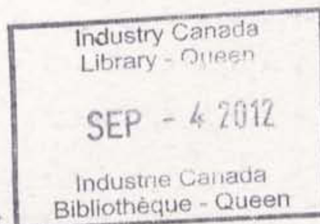
Industry Canada
Library - Queen
SEP - 4 2012
Industrie Canada
Bibliothèque - Queen

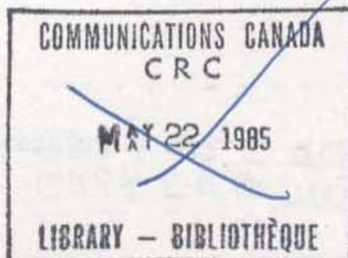
COMMUNICATIONS CANADA
CRC
MAY 22 1985
LIBRARY — BIBLIOTHÈQUE

CRC REPORT NO. 1298

October 1976
OTTAWA

CAUTION
This information is furnished with the express understanding that:
Proprietary and patent rights will be protected.

TK
5102.5
C673e
#1298
c.b

DD 5334856
DL 5334900

TABLE OF CONTENTS

ABSTRACT 1

1. INTRODUCTION 1

2. EXPERIMENTAL PROCEDURE 2

3. RESULTS AND DISCUSSION 4

3.1 Effect of HCl Concentration 4
3.1.1 Electrical Effects 4
3.1.2 Structural Effects 6

3.2 Effect of the Wafer Orientation 9

3.3 Effect of the Introduction of Helium During "HCl Oxidation". . . 9

3.4 The Effect of Annealing 9

3.5 Effect of the Various Oxidation Processes 12

3.6 Effects on Metallizations 14

3.7 Nature of Defects 14

4. CONCLUSIONS 20

5. ACKNOWLEDGEMENTS 22

6. REFERENCES 22

APPENDIX A - HCl-Oxides Processing 23

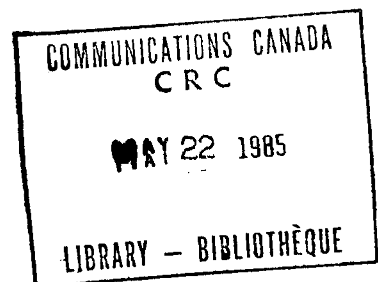
COMMUNICATIONS CANADA
CRC
MAY 22 1985
LIBRARY – BIBLIOTHÈQUE

THE STRUCTURE OF HCl DOPED SILICON OXIDES AND OF THE OVERLAYING METALLIZATION

by

M. Bouchard, W.A. Hartman and R.M. Kuley

ABSTRACT

The addition of chlorine during processing improves the dielectric properties of silicon dioxide by reducing the concentration of mobile ions in the oxide. Since about 1973 the industry has adopted an optimum value of approximately 4 vol % HCl:O_2 because of possible detrimental effects at higher concentrations of chlorine. We have found quantitatively that at higher concentrations of chlorine (e.g. 10 vol % HCl:O_2 mixture) the oxide surface becomes irregular and the excess chlorine forms pockets within the oxide. This work characterizes these oxide defects and shows that their number, size and distribution are influenced by the chlorine concentrations, the processing sequence, the cooling rate following the oxidation, and the wafer orientation. The oxide defects also cause a local lifting of most metallizations and can cause pitting of aluminum. These reliability hazards can be avoided by careful choice of processing parameters.

1. INTRODUCTION

The migration of positive ions in thin SiO_2 films is a major cause of electrical instabilities in MOS devices [1]. The introduction of chlorine-containing species during the thermal oxidation of silicon wafers has been reported to improve the electrical stability of the SiO_2 films by the immobilization of contaminants such as sodium [2-5]. In the cases of the "HCl oxides" and "Cl_2 oxides", the gases involved are very corrosive in the

presence of small amounts of water vapor and can be deadly to humans and cause corrosion of laboratory equipment if not vented properly. There is very little information available on the potential corrosion damage caused to MOS devices by the chlorine-bearing species [6].

The purpose of this work is to investigate the detrimental effects caused by the addition of various amounts of chlorine during the oxidation of silicon. We have studied the structural damage to silicon, silicon dioxide and overlaying metallizations, using electron metallography and microanalysis. In addition, the electrical stability of these oxides was investigated, in order to assess the quality of the SiO_2 films produced by our process, and to attempt to relate the increase in stability of the films grown in the presence of chlorine to the onset of structural damage.

2. EXPERIMENTAL PROCEDURE

Both <100> and <111> oriented n-type silicon wafers of 1-2 Ω-cm resistivity were cleaned just before oxidation as follows:

5 minutes etch in hot (70°C) HNO_3
10 minutes rinse in DI H_2O
1 minute etch in 10% HF: H_2O
10 minutes rinse in DI H_2O
Blow drying with N_2

The oxidation furnace was cleaned with a 10% (volume ratio) $HCl:O_2$ mixture for 45 minutes at the start of each day of processing. The oxidation temperature was maintained at 1150°C and the total flow rates were one l/min. for $HCl:O_2$ mixtures and 600 ml/min. for nitrogen. The gases were UHP grade and both factory mixtures and in-house mixtures were used to obtain concentrations of up to 10% $HCl:O_2$ and 3% $Cl_2:O_2$. In general, the samples were gradually transported to and from the hot zone of the oxidation furnace over a period of 1 minute in order to minimize thermal shock [3]. The standard chlorine oxidation process consisted of:

10 minutes of oxidation in dry O_2
18 minutes of oxidation in $HCl:O_2$ mixture (or $Cl_2:O_2$)
2 minutes of oxidation in dry O_2
10 minutes of *in situ* annealing in pure nitrogen

This process is described in the text as the HCl 10/18/2/10 process, and several modified processes were also investigated (see Table 1). The oxidized wafers were then stored under clean conditions until metallized by sputtering or electron beam evaporation. Two wafers of each orientation were processed during each oxidation, one of which was fully metallized on one side only, photolithographically etched into a simple pattern, and inspected for structural damage. Circular MOS capacitors were produced on the second wafer by partial metallization through a mask of the front surface and full metallization of the back. The latter wafer was used for capacitance-voltage measurements of the type described by Grove [7], to determine the mobile ion content of the layers grown in each oxidation run. The wafers were examined by scanning (SEM) and transmission (TEM) electron microscopy and by electron

beam microanalysis. The specimens for TEM analysis were prepared by back etching [8]. The technique consists of forming a hemispherical hole by jet-etching the back side of a small silicon sample with a solution of 15% HF in HNO_3 at 22°C while protecting the metallized face. The etching stops at the $Si-SiO_2$ interface, leaving an electron-transparent blanket of SiO_2 and metallization.

The technique for determining the mobile ion concentration in the oxide layer of a MOS capacitor is based upon measurement of the shift in flat-band voltage of the capacitor when a bias voltage is applied at elevated temperatures [9]. Typical high-frequency capacitance-voltage characteristics for MOS capacitors on n-type silicon are shown in Figure 1. It can be seen that a bias-temperature stress of $+10^6$ V/cm (metal electrode positive) at 250°C for five minutes, produces a negative drift of the voltage V_{FB} corresponding to the flat-band capacitance C_{FB}. A subsequent similar negative bias-temperature stress on the same device produces a positive drift of V_{FB}, which recovers almost to its original room temperature value. The movement of positive ions under the influence of the applied electric field is responsible for this shift in the C-V curves. The value of Q_o/q, the effective number of mobile ion charges per cm^2 at the oxide-silicon interface, can be calculated from the flat-band voltage shift ΔV_{FB}.

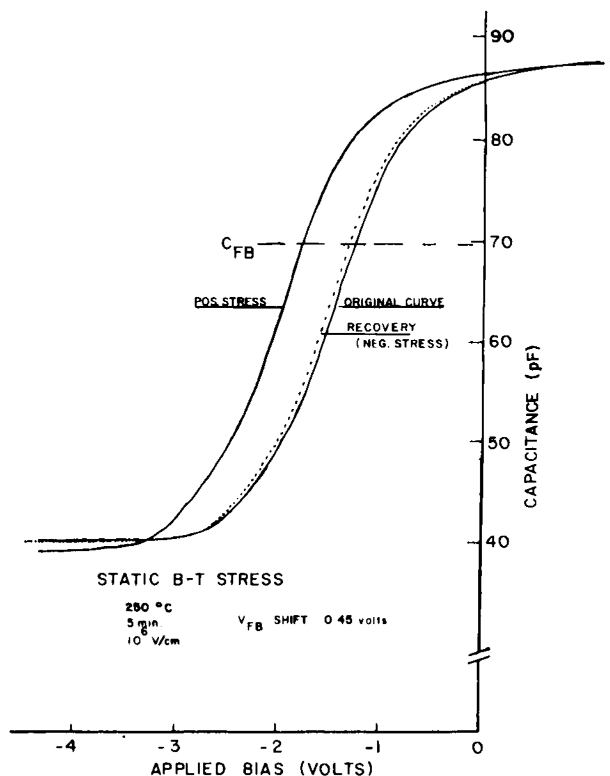

Figure 1. Capacitance-voltage Characteristics of MOS Capacitors on n-type Silicon, Showing Effect of Bias-Temperature Stressing

The bias-temperature stressing of the oxide samples was performed using a static charging technique [10], with field strengths of the order of $\pm 10^6$ V/cm for five minutes at 250°C. The voltage shift ΔV_{FB} was measured directly with a semi-automatic measurement facility based upon a Hewlett-Packard 2570A coupler/controller under program control of a Hewlett-Packard 9810A calculator. Included in this system is a Boonton 71AR capacitance meter, with which high-frequency (1 MHz) capacitance measurements were made.

The Q_o/q values such as those plotted in Figure 2 are averages resulting from measurements on five capacitors on each wafer examined.

3. RESULTS AND DISCUSSION

3.1 EFFECT OF HCl CONCENTRATION

3.1.1 Electrical Effects

The oxides grown with increasing HCl concentrations show a trend towards lower mobile ion content, with a sudden reduction in the region of 6-8% HCl content, especially for the <100> wafers. Results for the standard oxidation process are shown in Figure 2(a) for <111> oriented wafers and in Figure 2(b) for <100> wafers. Values of Q_o/q observed ranged from 9×10^{10} cm^{-2} for oxides with no HCl content to 1×10^9 cm^{-2} for 10% HCl content, with a slight rise to about 1.5×10^{11} cm^{-2} at 4% HCl content. There appeared to be little orientation effect on the passivating quality of the HCl oxide growth process, at least to 8% HCl content; it was not possible to obtain usable data at 10% $HCl:O_2$ for <100> wafers.

It is believed that the larger scatter of the results for <111> wafers than for <100> wafers comes from the fact that more wafers of the former type were tested and it reflects small variations caused by processing of individual wafers.

We also oxidized using $Cl_2:O_2$ mixtures and found that all values of Q_o/q were of the order of 1×10^{12} cm^{-2} for chlorine concentrations from 1-3% $Cl_2:O_2$.

The increase in the mobile ion concentration around 2-4% $HCl:O_2$ concentrations could have arisen from a higher level of ionic contamination introduced at some stage in the processing of those oxides. Because each group of oxide samples was metallized on different days, this processing step is felt to be the likeliest source of the increased contamination, considering that, if the oxidation system has been well-cleaned with HCl, the subsequent metallization is the major source of ionic contamination in the fabrication of MOS capacitors [2].

Occasionally, for oxides grown with higher concentrations of HCl, negative values of Q_o/q were obtained, indicating a shift of V_{FB} after negative stress in the same direction as after positive stress. Upon plotting complete C-V curves for capacitors representative of each of the HCl concentrations, it was found that it was not a shift in V_{FB} that was occurring after negative

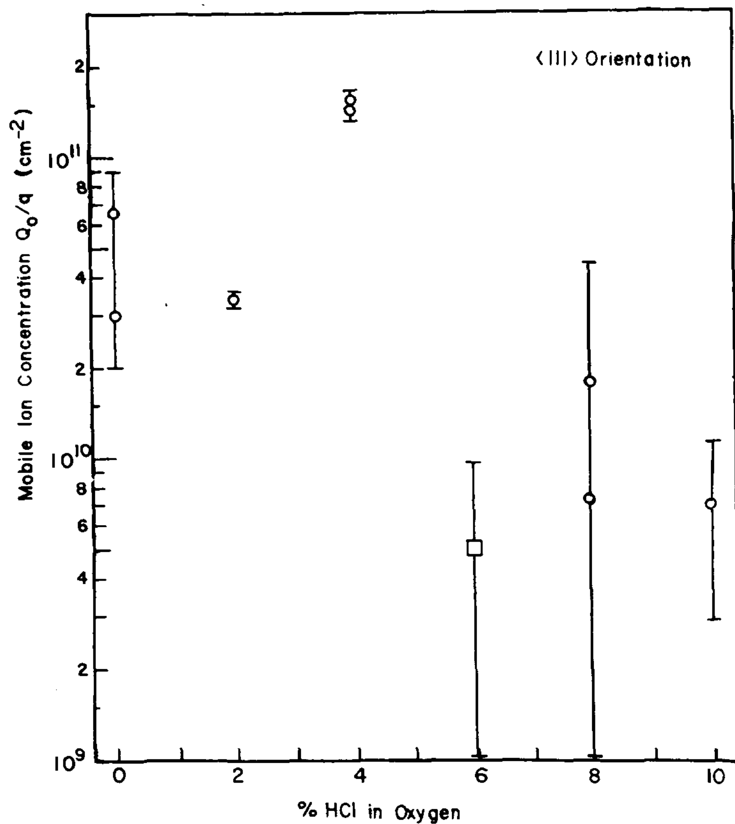

(a) For oxides on <111> wafers. □ values of Q_0/q obtained by alternate method discussed in Section 3.1.1.

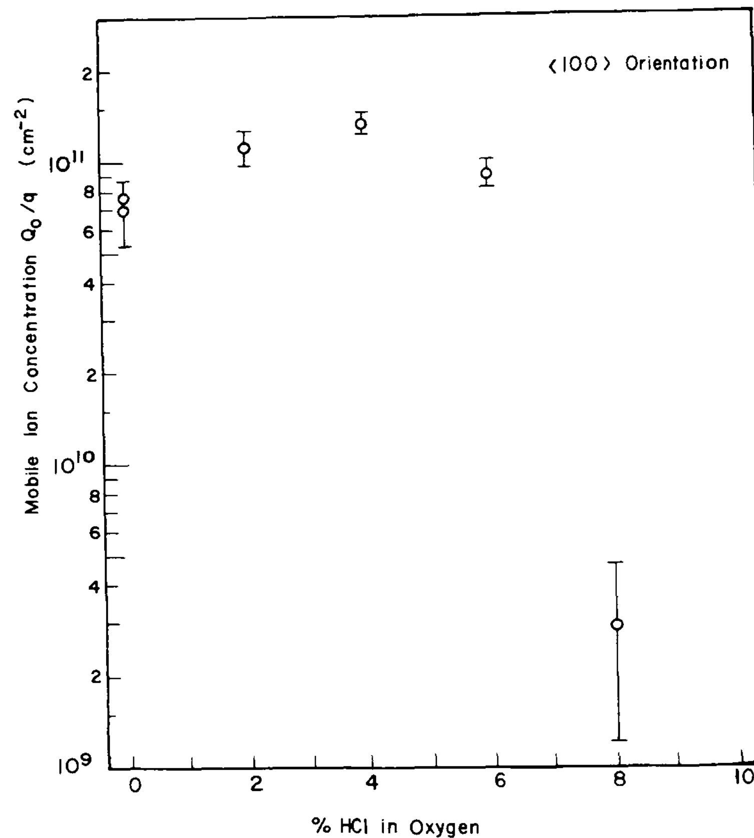

(b) For <100> wafers.

Figure 2. Mobile Ion Concentration of HCl Oxides as a Function of HCl Concentration. Averages and Uncertainties are Shown.

stress, but a decrease in the slope of the C-V characteristics in the vicinity of C_{FB}. This change in slope is shown in Figure 3. Typical C-V curves for a 2% HCl oxide are shown in Figure 3(a); the change in slope after negative stress is negligible. The curves in Figure 3(b), for a 10% HCl oxide, show the stretching-out effect on the C-V characteristic after negative stressing; for such an oxide, the data analysis program would indicate a shift in V_{FB} that would appear to be due to motion of negative ions.

Because the change in slope of the C-V curves after negative stress partially masked the effect of ionic motion and because the degree to which the slopes were affected was not uniform across a particular wafer, there was a large amount of scatter in the values of Q_o/q for oxides with HCl content in the range 6-10%. For those few capacitors with a negative value of Q_o/q, an upper limit for the mobile positive ion content could be calculated using the shift in V_{FB} between the value measured at room temperature and that observed after positive stress. In this way, Q_o/q for 6% HCl content oxide on <111> oriented wafers was found.

Distortions in C-V curves similar to the change in slope reported here have been related to the creation of fixed positive charge and fast surface states at the Si-SiO_2 interface [6, 11]. Such interface states are also formed under the action of negative bias-temperature stress [12], but the role of chlorine in enhancing creation of interface states under stress has not been noted specifically.

According to a model proposed by Deal for charge effects in SiO_2 [6], fast surface states are formed by the breaking of silicon-oxygen bonds at the silicon surface. This could be brought about by the application of a negative field across the oxide. Therefore, assuming that charge effects in SiO_2 are related to silicon bond structure and its defects, the presence of chlorine could be expected to distort the structure or affect it in a way that leads to increased formation of defects. As will be seen from the discussions in following sections of this report, there is evidence of such defect formation. Further work is needed before more detailed explanations of the electrical effects can be made.

3.1.2 Structural Effects

The above electrical results show a sudden decrease in the effect of mobile ions at 6% to 8% HCl:O_2. This trend was also reported by Kreigler *et al* [13]. These results indicate that it would seem to be advantageous to incorporate more than 6% (vol.) of HCl into the oxidizing atmosphere for high stability oxides. However, the corresponding scanning electron micrographs of "HCl oxides" in Figure 4 reveal the presence of defects in the oxides processed with more than 6% HCl. The defect density remains constant with increasing HCl concentration above 6% but the contrast increases with HCl concentration. The defective "10% HCl oxides" show large defects approximately 1μm. in diameter, surrounded by a band of smaller defects whose diameter decreases with increasing distance from the centre of the main defect. The nature of these oxide defects will be treated in Section 3.8.

We have observed two types of defects in metallizations overlaying highly doped "HCl oxides". The most common defect observed is the local lifting of the metal in areas just above the defects in the oxides thus generating a

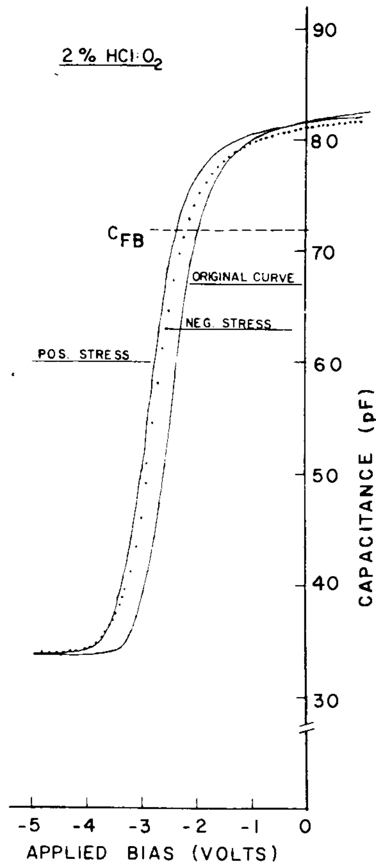

(a) For 2% HCl:0_2 concentration.

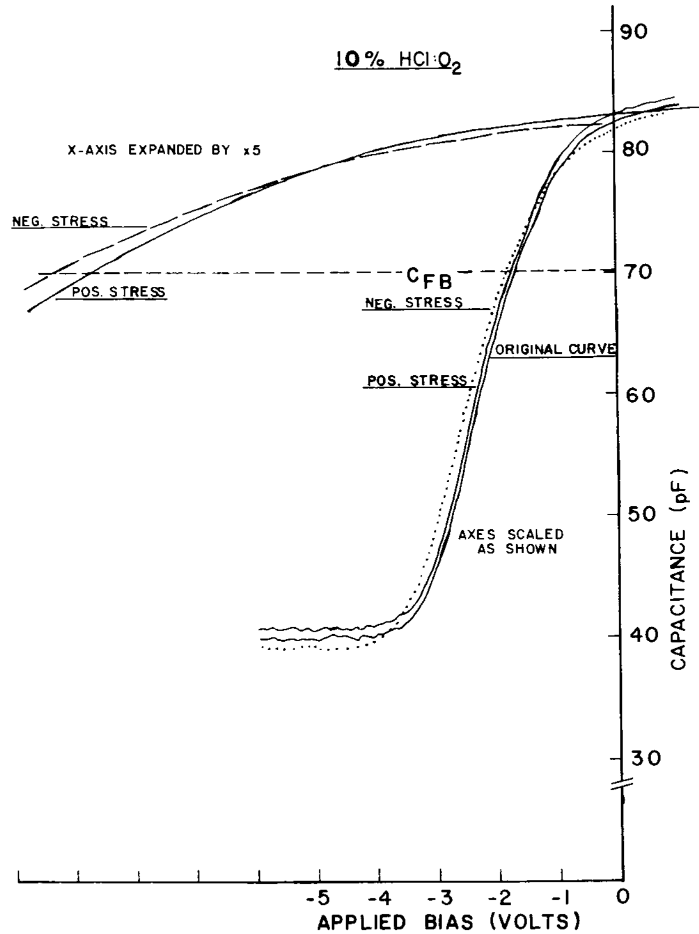

(b) For 10% HCl:0_2 concentration.

Figure 3. Effect of HCl Content of Oxide Layer on Slope of C-V Characteristics of MOS Capacitor after Negative Bias-Temperature Stress

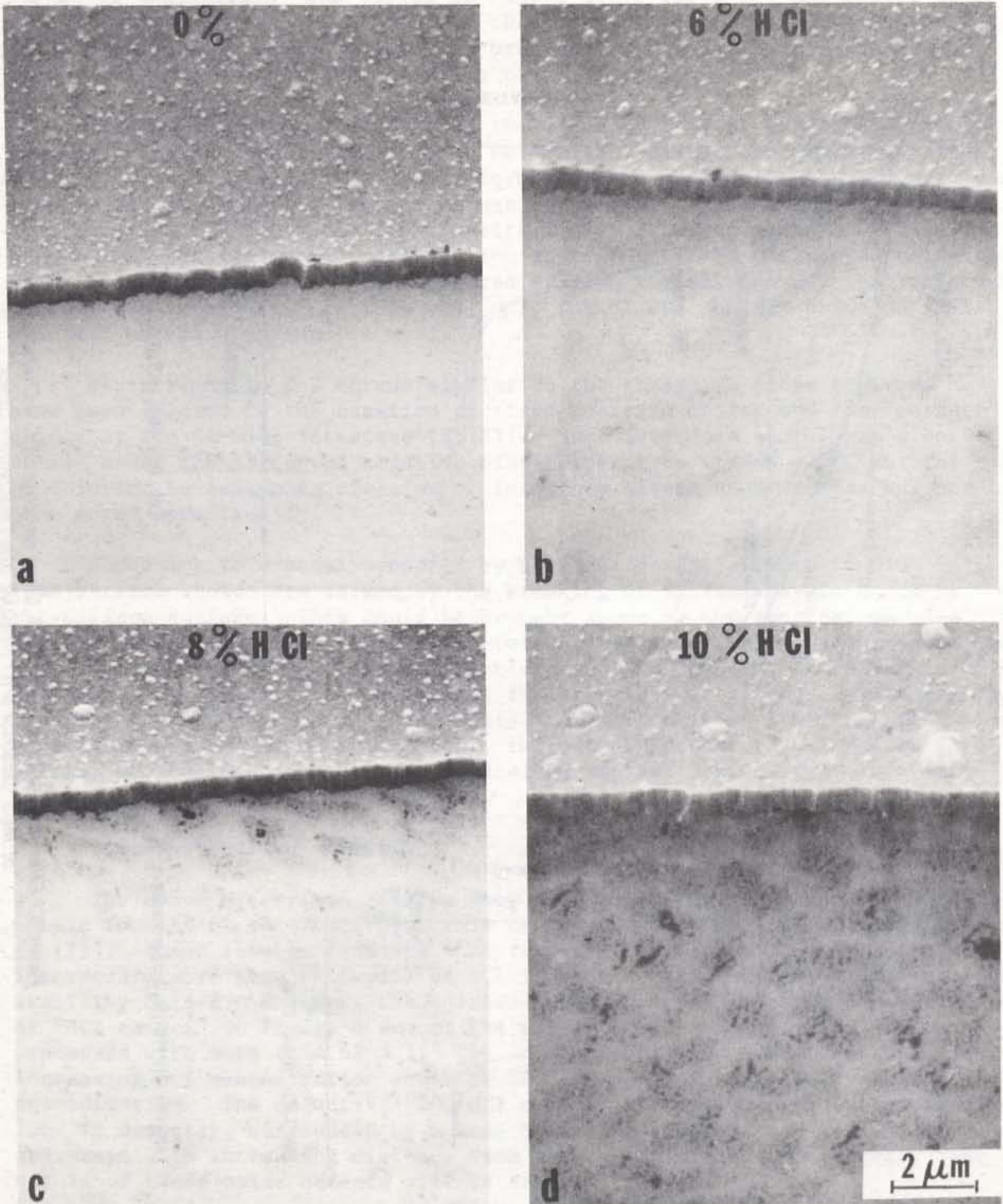

Figure 4. SEM photographs of oxides (lower part) processed with increasing $HCl:O_2$ volume ratio metallized with 5000 Å thick aluminum (upper part). Note the heterogeneous oxides at high-HCl concentration.

blistering effect. The amount of blistering increases with the $HCl:O_2$ ratio during oxidation and also with post-metallization annealing at 450°C (see Figure 5). The blistering is better observed at high angle of incidence in the SEM as illustrated in Figure 6. In non-annealed <111> oriented samples, oxidized using the standard 10/18/2/10 process, blistering was observed only with the "10% HCl oxides" (see Figure 6). The most severe blistering observed was associated with a Ti-Al-Ti sandwich metal layer annealed for two hours at 450°C and shown in Figure 5.

The second type of "chlorine-induced" defect in metallizations is the localized pitting observed only after annealing at temperatures higher than 200°C (see Section 3.8). The "Cl_2 oxides" were processed with up to 3% (vol.) $Cl_2:O_2$ mixtures and no defects were observed either in the oxides or metallizations.

3.2 EFFECT OF THE WAFER ORIENTATION

The effects shown in Figure 4 on the <111> oriented wafers are less pronounced in the similarly processed <100> oriented wafers. Figure 7 shows the <100> oriented wafers processed with 0% to 10% $HCl:O_2$ mixtures. It can be seen that using the standard 10/18/2/10 "HCl oxidation" process, the defects in the oxides are noticeable only at the very high level of 10% HCl which compares to the 6% $HCl:O_2$ level for the <111> oriented wafers. No defects were observed in the metallizations under any of the standard HCl 10/18/2/10 processes or under any of the 0% to 3% Cl_2 oxidation on <100> oriented wafers.

3.3 EFFECT OF THE INTRODUCTION OF HELIUM DURING "HCl OXIDATION"

It has been suggested that an $HCl:O_2$ mixture diluted with helium also provides excellent passivation of the mobile ions [14, 15]. We have studied the influence of the dilution with helium of a 10% $HCl:O_2$ mixture, using <111> oriented wafers and the standard 10/18/2/10 process. The range of mixtures studied was from 9/1 of He/10% $HCl:O_2$ and 5/5 He/10% $HCl:O_2$. The results have shown that a mixture of approximately 6 parts He and 4 parts 10% $HCl:O_2$ appears to be the maximum level for homogeneous oxides. The SEM micrographs obtained at high angle of observation failed to show any blistering or pitting of the aluminum metallization even after annealing at 450°C for 1 hour, for the helium mixtures studied.

3.4 THE EFFECT OF ANNEALING

SEM examination suggests that annealing of the "high concentration HCl oxides" does not affect the structure of the oxide defects introduced during oxidation. On the other hand, the corresponding metallizations become more defective with increasing annealing time. First, during annealing, the height of the local bumps or blisters in the metallization increases. This is illustrated in Figure 5 for the Ti-Al-Ti sandwich layer. In Figure 5, it can be seen that the blisters are located immediately above the defects in the oxides. Second, the annealing generates pits in the metallization (see Figures 5 and 8). Although less frequently observed than blistering, the phenomena of pitting does not always relate to an underlaying "HCl defect" in the oxide. The nature of the defects will be further discussed in Section 3.8.

Figure 5. SEM Photographs of a 10% HCl 18/10/2/10 Oxide and the Overlaying Ti-Al-Ti Metallization Showing
(a) the absence of metal lifting before annealing and
(b) the local lifting and pitting of the metallization after annealing.

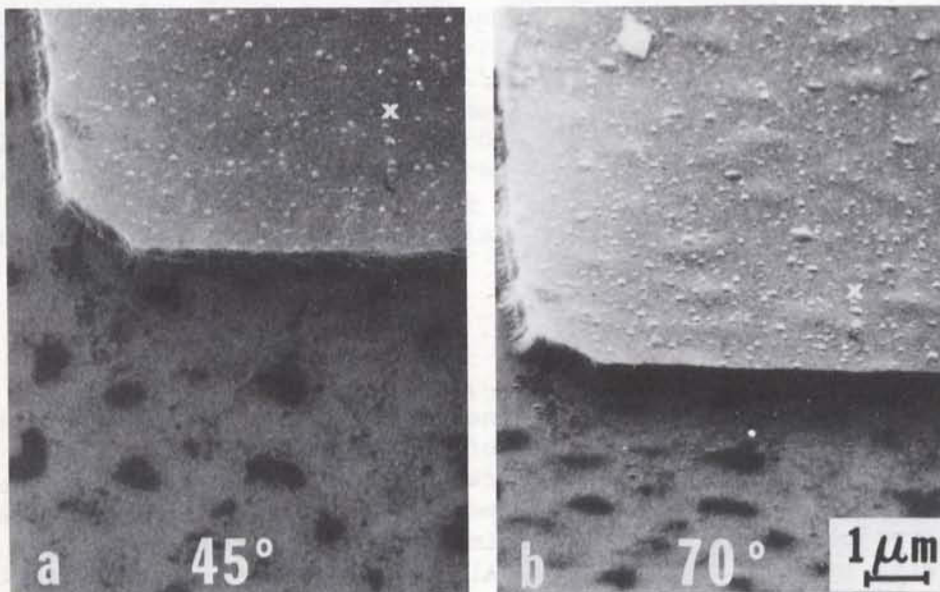

Figure 6. SEM Photographs of a 5000 Å Thick Aluminum Metallization Covering a 10% HCl 18/10/2/10 Oxide and Showing the Same Area (Marked X) at Two Angles of Observation in the SEM. The Blistering is Only Visible when Observed at 70° in the SEM (see (b)).

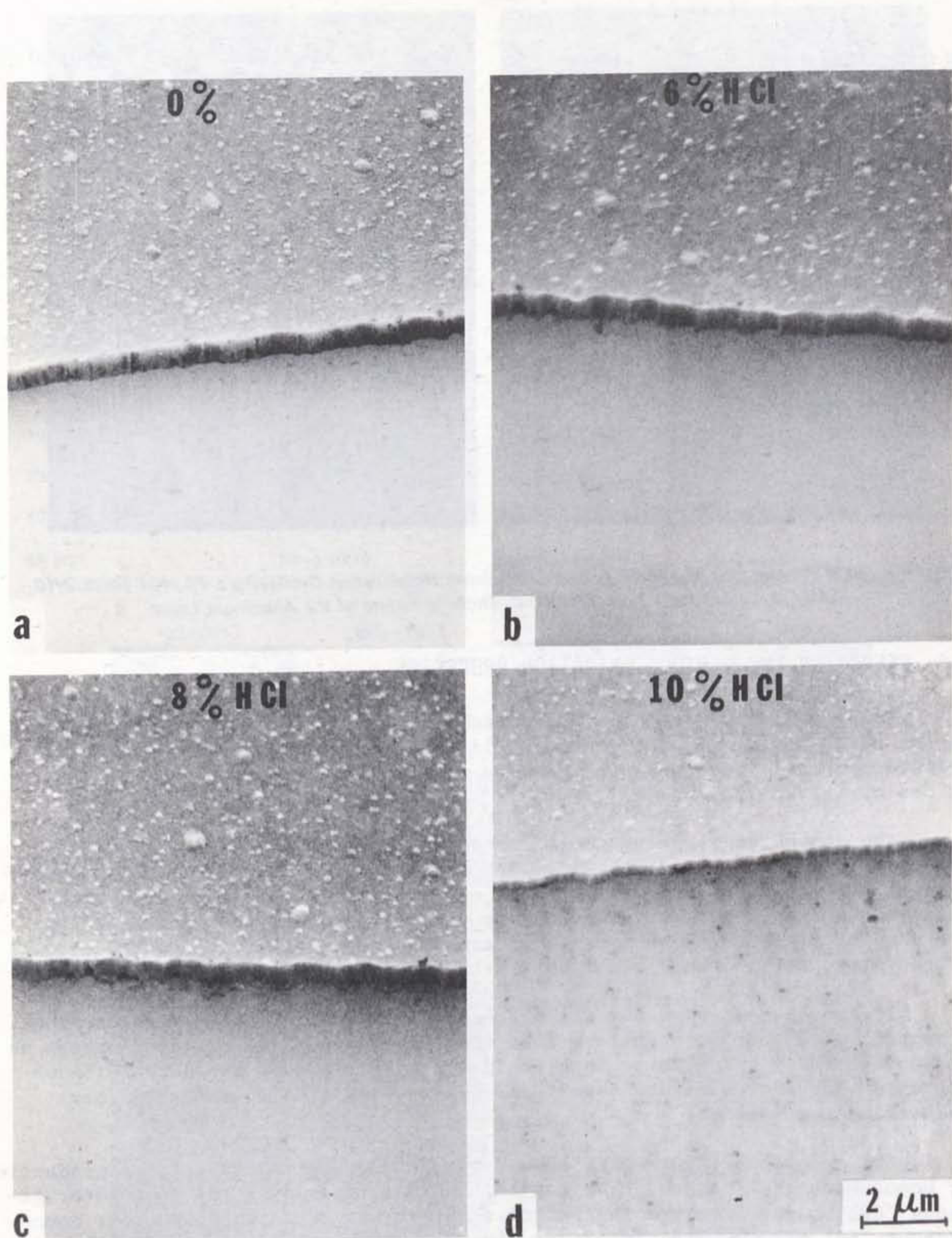

Figure 7. SEM Photographs of <100> Wafers Oxidized Using the 18/10/2/10 Process with Various HCl Concentrations from 0 to 10% (Vol.). Defects in the Oxides are only Observed After the 10% HCl Process

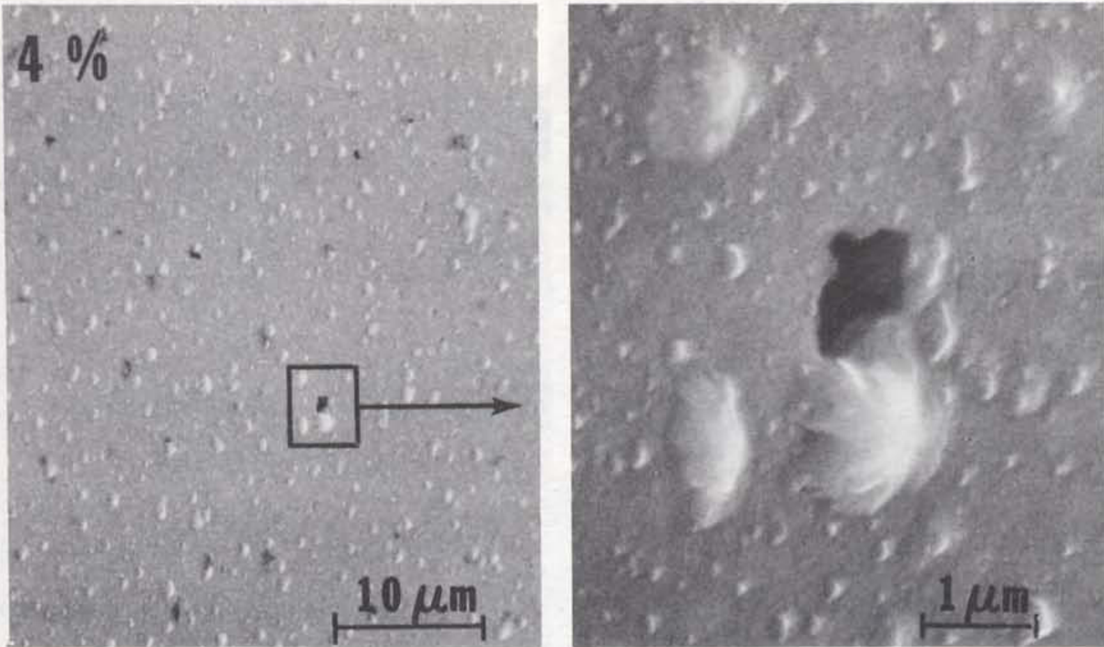

Figure 8. SEM Photographs of a 5000 Å Thick Aluminum Metallization Overlaying a 4% HCl 10/18/2/10 Oxide, Annealed for 1 Hour at 450° C, Showing Pitting of the Aluminum Layer.

3.5 EFFECT OF THE VARIOUS OXIDATION PROCESSES

We have investigated the influence of various HCl oxidation processes on the structure of the oxide and metallizations both, on <111> and <100> oriented wafers. The processes studied and the quality of the resulting oxides are given in Table 1.

The composite Figure 9 shows the structure of the oxides for some processes of Table 1 on <111> and <100> oriented wafers. The rows illustrate the influence of the oxidation process on the various wafers whereas the columns illustrate the influence of the various processes on one wafer-type. The density of the oxide defects indicates that the structural damage caused by the processes increases from bottom to top of the figure.

It can be seen that for all processes, the "HCl oxides" grown on <100> oriented wafers are more uniform than those grown on <111> oriented wafers as in Section 3.2. Furthermore for each process, the figure shows that the 6% HCl oxides are more uniform than their 10% counterparts as expected from results in Section 3.1.

The composite figure also shows some processing limits for the production of homogeneous HCl oxides. The top left corner represents the most heterogeneous "HCl oxides" whereas the bottom right corner represents the most homogeneous "HCl oxides". An imaginary line from the bottom left to the top right of the figure is the approximate boundary for the observation of the visual defects. The processing variables are discussed in more details in Appendix A.

TABLE 1

Concentration	Process Sequence (min.) dry O_2/HCl:O_2/dry O_2/N_2	Process Type	Oxide Defects Visible by SEM
0% HCl	30/0/0/10	non-HCl oxidation	clean oxides
0% to 10% HCl	10/18/2/10	standard process	progressively more defective oxides above 6% on <111> wafers and above 8% on <100> wafers
1% to 3% Cl_2	10/18/2/10	standard process	clean oxides
10% HCl	10/20/0/0	modified process	very defective oxides
6% HCl	10/20/0/0	modified process	defective oxides
10% HCl	10/20/0/0	modified process	very defective oxides
6% HCl	10/20/0/10	modified process	defective oxides
10% HCl	18/10/2/10	modified process	defective oxides only on <111> wafers
6% HCl	18/10/2/10	modified process	clean oxides
10% HCl	10/10/10/10	modified process	clean oxides
6% HCl	10/10/10/10	modified process	clean oxides

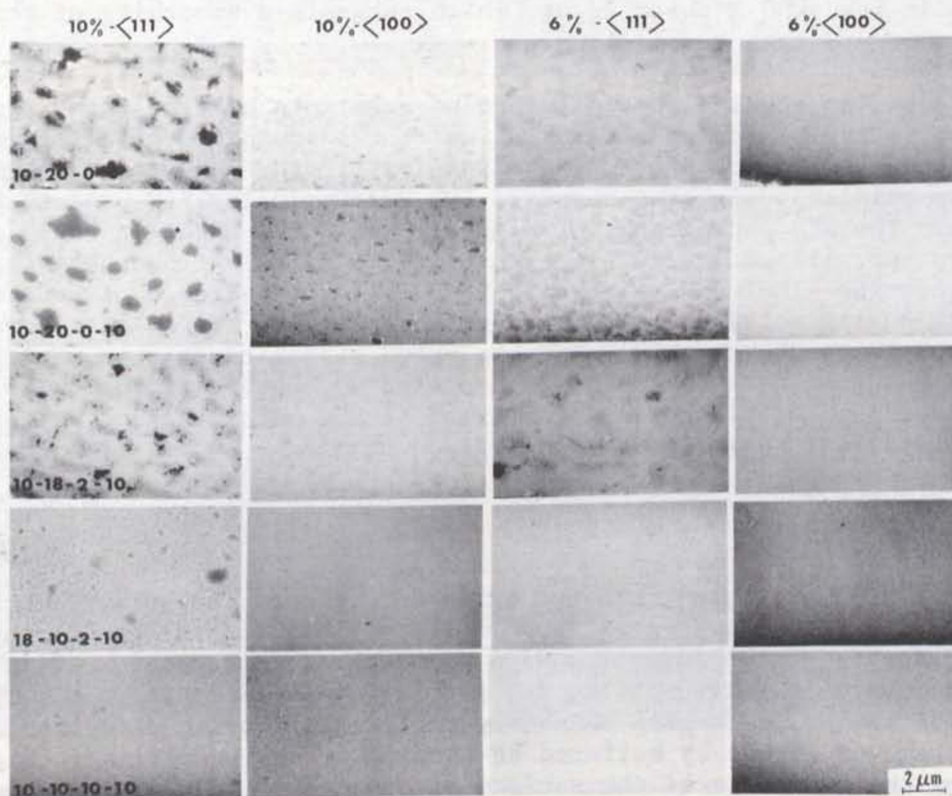

Figure 9. SEM photographs of HCl oxides on <111> and <100> wafers processed according to the indicated HCl concentration and oxidation sequence.

3.6 EFFECTS ON METALLIZATIONS

This series of experiments consisted of preparing the following metallizations on the standard 10% HCl 10/18/2/10 oxides grown on <111> oriented wafers.

(a) 500 Å Ti + 4000 Å Al + 500 Å Ti (by evaporation)

(b) 500 Å Ti + 5000 Å Al (by evaporation)

(c) 400 Å Si + 5000 Å Al (by evaporation)

(d) 500 Å Cr + 5000 Å Au (by evaporation)

(e) 500 Å Ti-W + 5000 Å Au (by sputtering)

The localized lifting of metallization was observed in all the above cases and it was enhanced after annealing at 450°C. This behaviour is illustrated in Figure 5 for the Ti/Al/Ti metallization.

We have also studied the influence of the thickness of the aluminum layer (200 Å - 5000 Å) on the nature of the defects in the metallization and found that at all aluminum thicknesses, the heavily doped "HCl oxides" produce blistering and that the post-metallization annealing enhanced it. In non-annealed samples, the blistering is more easily noticeable in the 200 Å thick layer than in the 5000 Å thick layer, which suggests a smoothing of the aluminum surface during evaporation.

We have also studied the influence of substrate heating (from room temperature to 270°C) during metallization on the incidence of metal defects caused by the presence of HCl during oxidation. Both <100> and <111> oriented wafers were oxidized using the standard 10% $HCl:O_2$ 10/18/2/10 process for this experiment. The SEM photographs of Figure 10 show non-annealed "HCl" and "non-HCl" oxides, metallized at two different temperatures. It has been observed that for both the <100> and <111> oriented wafers an increase of substrate temperature during metallization increases the surface roughness. However, a comparison between the "non-HCl" and the "HCl" oxides reveals no visible structural changes in the metallization caused by the incorporation of HCl during oxidation. No blistering or pitting of the metallization was observed even at the highest angle of SEM observation of 85°.

3.7 NATURE OF DEFECTS

It has been suggested that the oxide defects are irregularities in the oxide surface produced by the pitting of the silicon surface by HCl incorporated during oxidation [3]. The SiO_2 was removed in order to verify if the irregularities observed at the top surface of the SiO_2 layer were simply a replica of silicon etch pits caused by HCl etching during oxidation. The oxide was removed either by buffered HF etching or by ion milling. Figures 11 and 12 show the structure of the surface after etching to increasing depths in the oxides using buffered HF and ion milling respectively. In both cases, it can be seen that the shape of the oxide defects gradually changes as the oxide becomes thinner, suggesting that the defects are tapered and located

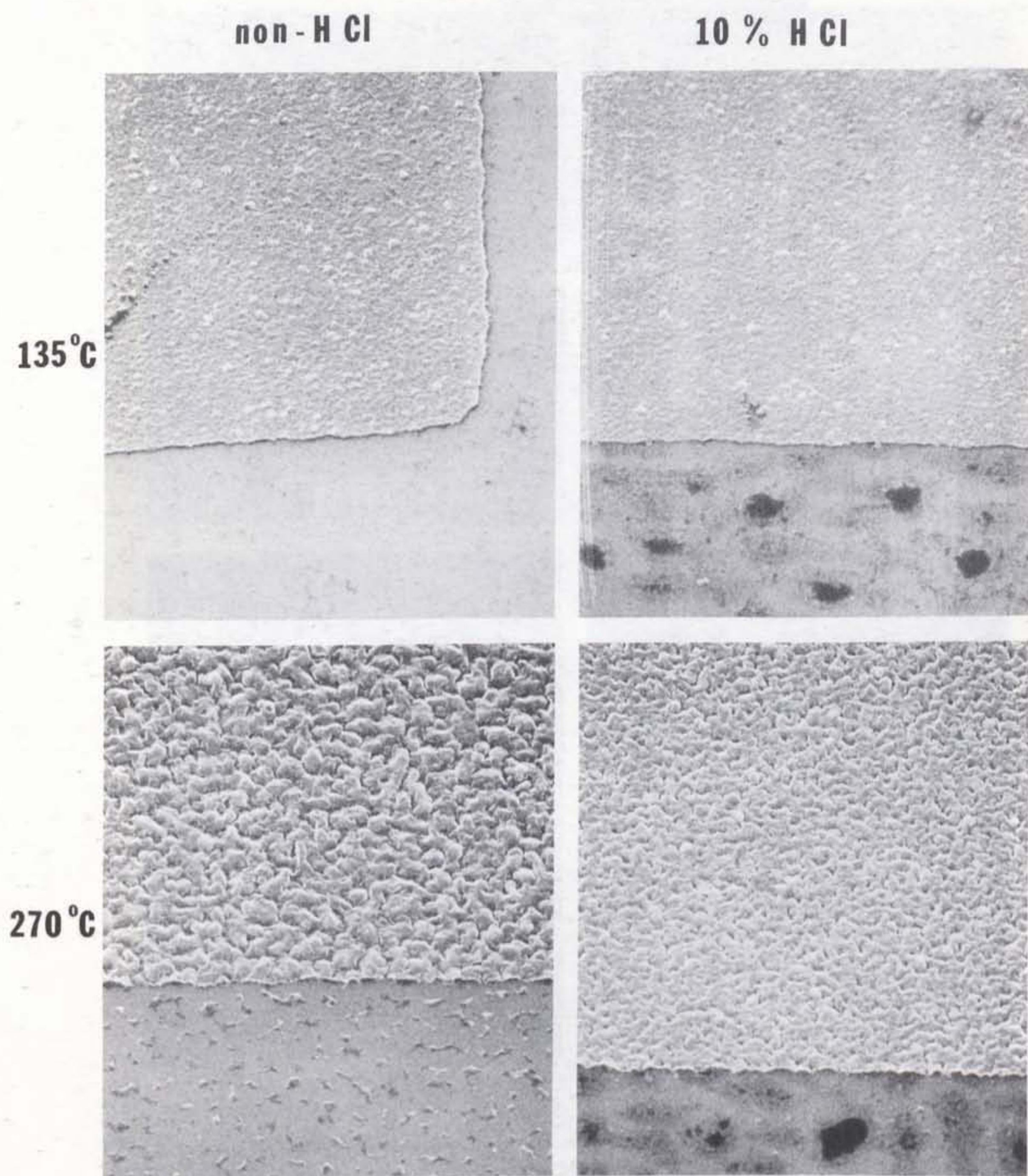

Figure 10. Effect of wafer temperature during deposition of aluminum metallization on non-HCl oxides and 10% $HCl:O_2$ 10/18/2/10 oxides on <111> wafers.
(a) Substrate temperature: 135°C.
(b) Substrate temperature: 270°C.

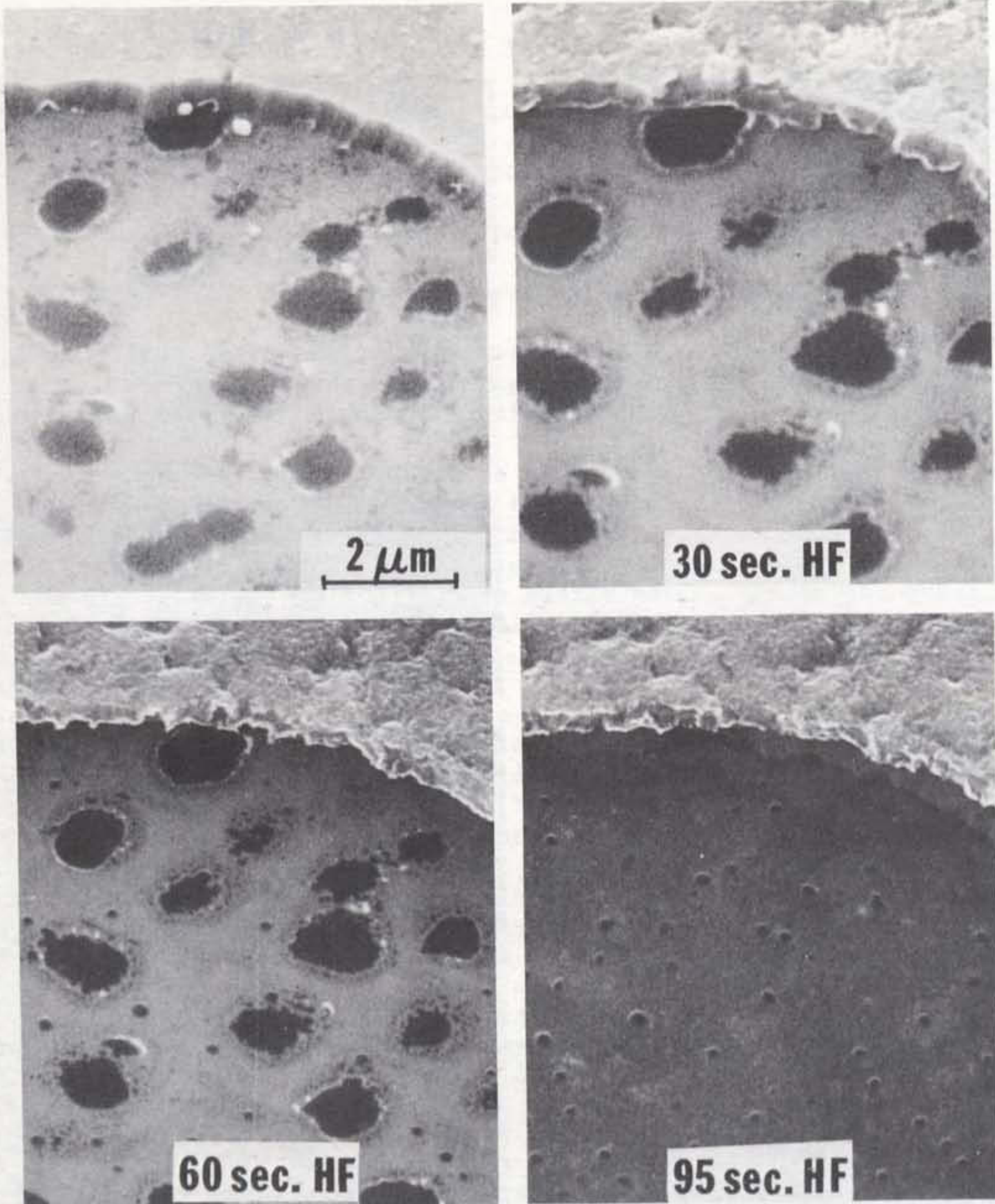

Figure 11. SEM photographs of etched silicon oxide grown on <111> wafers using the 10% $HCl:O_2$ 10/20/0/10 oxidation process.

(a) The as-oxidized wafer.

(b) After 30 seconds buffered HF etch.

(c) After 60 seconds etch.

(d) After 95 seconds etch.

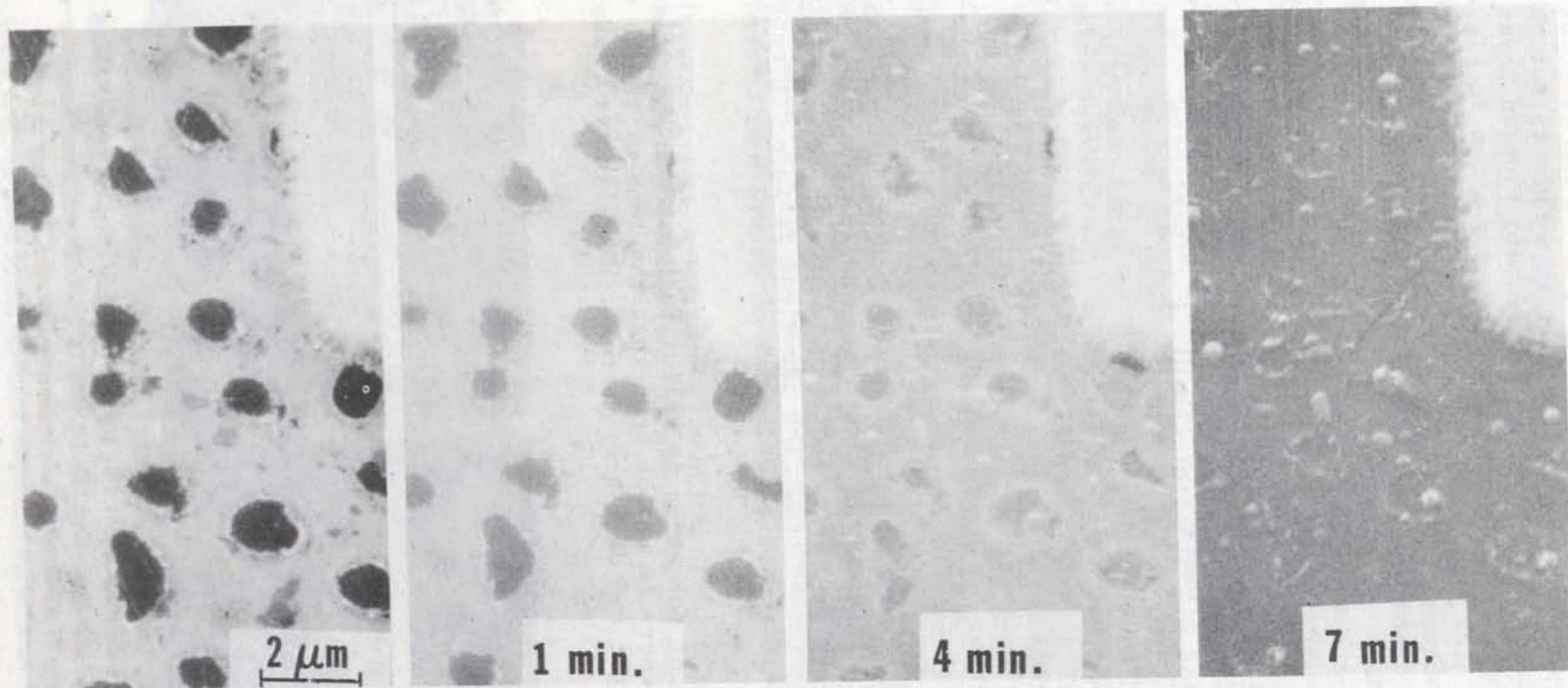

Figure 12. SEM photographs of ion-milled silicon oxide grown on <111> wafers using the 10% HCl :O_2 10/20/0/10 process.
(a) The as-oxidized wafer.
(b) After 1 minute ion-milling.
(c) After 4 minutes ion-milling.
(d) After 7 minutes ion-milling.

within the oxide. For the ion milled sample, Figure 12 does not indicate the as-grown condition of the silicon-oxide interface at the start of oxidation because of the constant shadowing during milling. This is not the case for buffered HF etching and Figure 13 shows a very thin tapered layer of SiO_2 obtained by HF etching of the non-homogeneous oxide shown in Figure 11. SEM observations at very high angles of incidence indicate that the thin SiO_2 layer contains flat bottom craters surrounded by a ridge [see Figure 13 (b), (c) and (d)]. These craters may be generated by variable etching rates on an initially flat surface or by an irregular surface. The photograph in Figure 13 (d) shows very shallow craters on the silicon surface believed to be caused by HCl etching of the silicon surface during the HCl oxidation. However, the depth of the silicon pits is estimated at less than 100 Å and this is far too small to produce the strong contrast observed on the oxide surface. It is therefore concluded that the defects are located within the oxide rather than being a replica of the Si-SiO_2 interface.

We have studied the heterogeneous oxide by fixed beam electron microprobe analysis and observed small variations in the chlorine concentration inside and outside the defects. Typical values for 10 seconds counting time were 8 counts per second (cps) inside, 3 to 4 cps outside and a background of 1 cps. This analysis suggests that the oxide defects contain approximately three times the amount of "chlorine-bearing species" found in the rest of the oxide.

Figure 14 shows a transmission electron micrograph of a "10% HCl:O_2 10/18/2/10 HCl oxide" illustrating five stages during the formation of the defects. The defects form by a nucleation and growth process similar to solid state phase transformations. The identical diffuse diffraction rings of Figure 15 reveal that the defects and the oxide are made of similar amorphous material.

The first stage of formation is well illustrated in the areas between well-defined defects where it can be seen that the tone of theses areas fluctuates between light and dark grey (see A). The lighter areas are believed

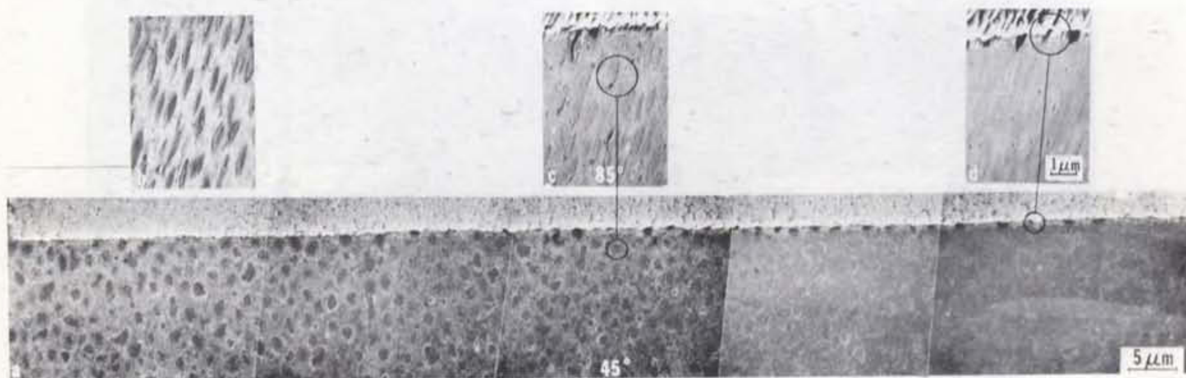

Figure 13. SEM photographs showing a thin SiO_2 layer obtained by chemical etching for 95 seconds in buffered HF (<111> wafer and 10% HCl:O_2 10/20/0/10 oxidation process).
(a) The thickness of the irregular oxide decreases to zero from left to right.
(b), (c) and (d) Selected areas of region shown in (a), obtained at higher angles of incidence.

Figure 14. Transmission electron micrograph of a 10% HCl:O_2 10/18/2/10 oxide on <111> silicon wafer, showing the nucleation and the growth of the chlorine-rich defects.

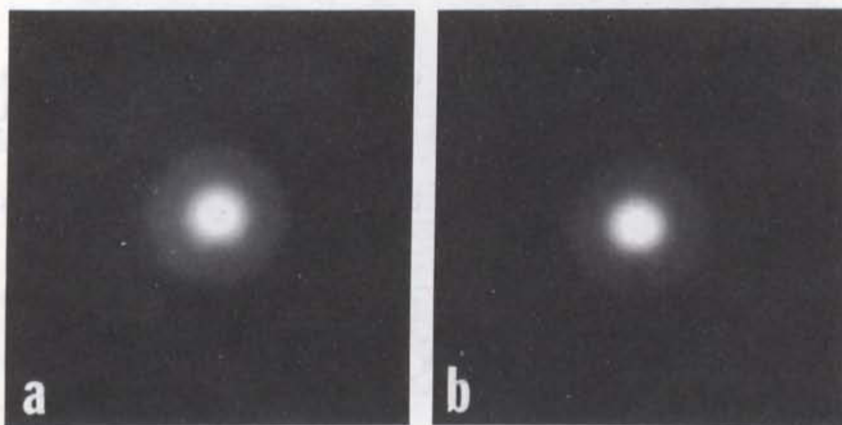

Figure 15. Diffuse diffraction rings obtained from the same sample as used for Figure 19.
(a) From within the chlorine-rich defect.
(b) From region outside the defect.

to reflect the early stage of formation of the chlorine-rich regions by the segregation of the chlorine-rich species at high temperature.

The area marked (B) shows the nucleation of small defects approximately 150 Å in diameter. These defects appear as well-defined white dots forming within lighter grey areas between the defects. These results suggest that the white dots form by the precipitation of chlorine-rich species from a supersaturated media. The area marked (C) shows the growth of a cluster of small defects by the widening of individual defects and by the formation of new 150 Å defects along the periphery of the cluster.

The area marked (D) shows the formation of the core of a larger defect by the clustering of the defects located near the centre of the cluster.

The large defects further grow by two mechanisms occurring within the peripheral belt of small defects. First, new small defects nucleate and grow at the outer periphery of the belt by the mechanisms previously described, thus increasing the size of the defect. Second, at the periphery of the core the growing small defects join the core by the process of clustering, thus increasing the size of the core. This is illustrated in the area marked (E) in Figure 14.

The above described mechanism of transformation takes place during cooling from the oxidation temperature (1150°C). This is illustrated in Figure 16 showing <111> oriented wafers oxidized using the standard 10% HCl 18/10/2/10 process and removed from the hot zone of the furnace at various rates. It can be seen that the size of the core and peripheral defects decreases with increasing cooling rate. This is indicative of the precipitation of the chlorine bearing species by diffusion during cooling from the oxidation temperature. At 1150°C, the SiO_2 absorbed the equilibrium concentration of chlorine-bearing species.

4. CONCLUSIONS

This work has shown:

(1) That increasing HCl concentration during oxidation tends to decrease the mobile ion concentration but also produces heterogeneities in oxidized <111> wafers when more than 6% HCl is incorporated in the oxidizing atmosphere.

(2) That the heterogeneity threshold for similarly processed <100> wafers is between 8% and 10% $HCl:O_2$ concentration.

(3) That the defects in the oxide represent heterogeneities in the distribution of the chlorine-bearing species within the oxide. The defects nucleate and grow to 1 μm in diameter during cooling from the oxidizing temperature by diffusion from a supersaturated solution of chlorine in the oxide.

(4) That increasing the post-oxidation cooling rate decreases the incidence of defects in the oxide.

(5) That the introduction of a partial pressure of helium during HCl oxidation decreased the incidence of oxide defects.

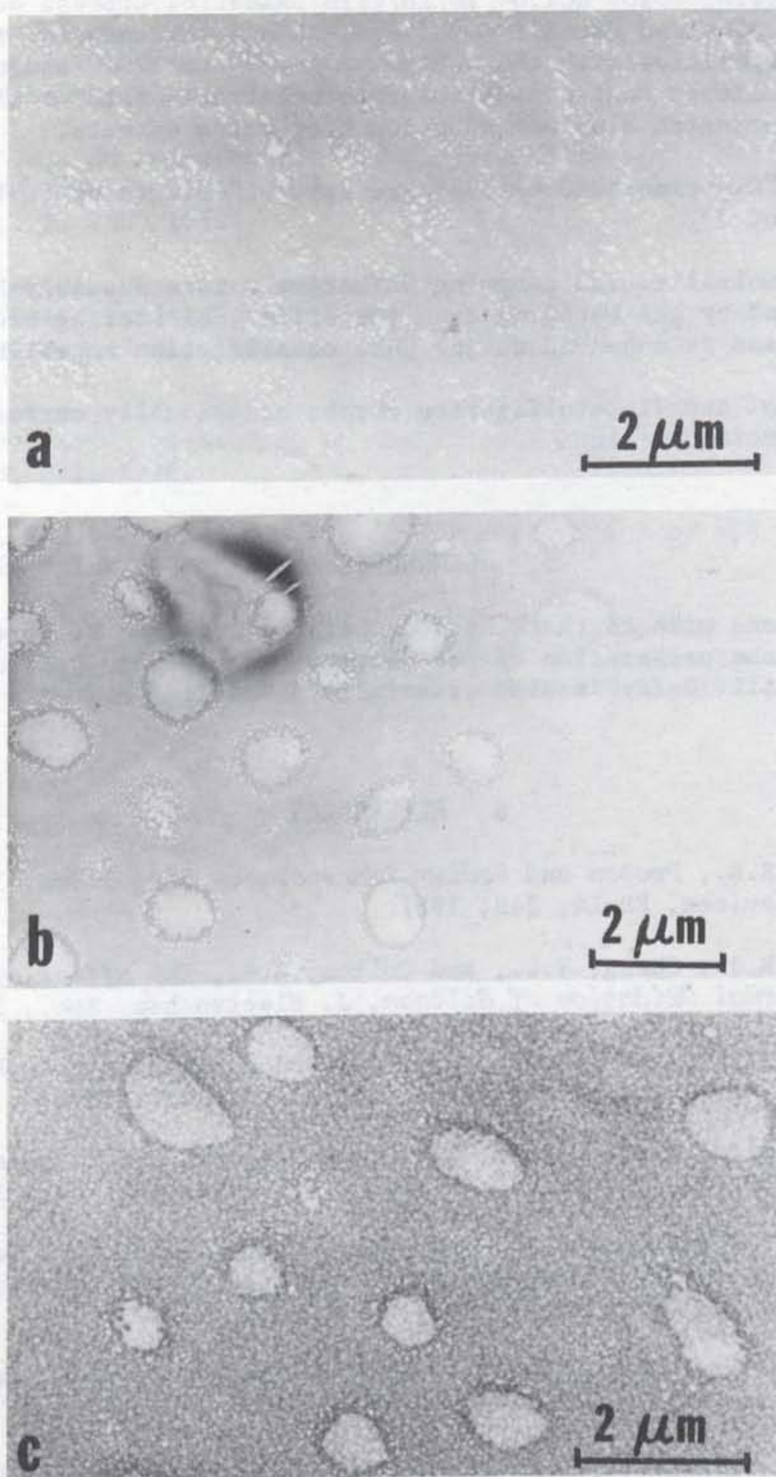

Figure 16. Transmission electron micrographs of similarly-processed 10% HCl:0_2 10/18/2/10 oxides on <111> oriented wafers, cooled from the oxidation temperature 1150°C to room temperature at different rates. Cooling times are:

(a) few seconds
(b) one minute
(c) ten minutes

(6) That following a 10% $HCl:O_2$ 10/18/2/10 oxidation process on <111> wafers, blistering was observed for all metal systems and thicknesses studied except for aluminum deposition with the substrate heated to 170°C and/or 230°C. It is therefore believed that deposition onto substrates held at elevated temperatures increases aluminum adhesion over oxide defects.

(7) That the "Cl_2-processed oxides" are free of defects up to the maximum level studied of 3%.

(8) That the metallization covering defective oxides possibly blistered by pressure exerted by gas escaping from the oxide. Blistering occurs during metallization and is enhanced during post metallization annealing at 450°C.

(9) That the Al and Ti metallization may be occasionally corroded by chlorine-rich gas, producing pitting.

5. ACKNOWLEDGEMENTS

The authors wish to thank Mrs. J. Legault and Mrs. R. Worm for their assistance in the preparation of the samples used in this project. Encouragement from Dr. A.L. Barry is also gratefully acknowledged.

6. REFERENCES

1. Hofstein, S.R., *Proton and Sodium Transport in SiO_2 Films*, IEEE Trans. Electron Devices, ED-14, 749, 1967.

2. Kriegler, R.J., Cheng, Y.C., and Colton, D.R., *The Effect of HCl and Cl_2 on the Thermal Oxidation of Silicon*, J. Electrochem. Soc., 119, 388, 1972.

3. Hirabayashi, K., and Iwamura, J., *Kinetics of Thermal Growth of HCl-O_2 Oxides on Silicon*, J. Electrochem. Soc., 120, 1595, 1973.

4. Van der Meulen, Y.J., Osburn, C.M., and Ziegler, J.F., *Properties of SiO_2 Grown in the Presence of HCl or Cl_2*, J. Electrochem. Soc., 122, 284, 1975.

5. Declerck, G.J., Hattori, T., May, G.A., Beaudoin, J., and Meindl, J.D., *Some Effects of 'Trichloroethylene Oxidation' on the Characteristics of MOS Devices*, J. Electrochem. Soc., 122, 436, 1975.

6. Deal, B.E., *The Current Understanding of Charges in the Thermally Oxidized Silicon Structure*, J. Electrochem. Soc., 121, 198C, 1974.

7. Grove, A.S., *Physics and Technology of Semiconductor Devices*, John Wiley and Sons, 1967, pp. 271-276.

8. Bouchard, M., *Electron Microscopy of the Ti-Al Thin Films*, Proc. 8th Int. Congress on Electron Mic., Canberra, 1974.

9. Grove, A.S., *Physics and Technology of Semiconductor Devices*, pp. 337-340.

10. Barry, A.L., Hum, R.H., and Kuley, R.M., *A Rapid Method of Bias-Temperature Stressing Using a Static Charge Technique*, Paper presented at Autumn symposium of the Ontario/Quebec section of the Electrochemical Society, Ottawa, November, 1974.

11. Terman, L.M., *An Investigation of Surface States at a Silicon/Silicon Oxide Interface Employing Metal-Oxide-Silicon Diodes*, Solid-State Electron., 5, 285, 1962.

12. Goetzberger, A., Lopez, A.D., and Strain, R.J., *On the Formation of Surface States during Stress Aging of Thermal Si-*SiO_2 *Interfaces*, J. Electrochem. Soc., 120, 90, 1973.

13. Kriegler, R.J., Aitken, A., and Morris, J.D., *The Use of HCl Passivation in the Processing Technology of MOSFET Devices*, J. Japan Soc., Appl. Phys., 43, 341, 1974.

14. Kriegler, R.J., *The Role of HCl in the Passivation of MOS Structures*, Thin Solid Films, 13, 11, 1972.

15. Kriegler, R.J., Morris, J.D., and Colton, D.R., *Sodium Ion Movement in HCl Passivated* SiO_2 *Films*, Paper presented at the Electrochemical Society Meeting, Miami Beach, Florida, October 8-13, 1972.

APPENDIX A

HCl - Oxides Processing

The two most severe processes are the 10/20/0/0 and the 10/20/0/10 (the top two rows of Figure 9). These two processes differ by the 10 min. nitrogen anneal at the end of the latter process. The figure shows that this 10 min. anneal does not appreciably change the structure of the oxide defects. These two processes produce well defined defects of high contrast in 10% HCl oxides both on <111> and <100> oriented slices. Some of these defects are also characterized by a slight ridge along the perimeter of the dark areas.

The composite Figure 9 also suggests that a two minute dry O_2 oxidation following the long 10% $HCl:O_2$ oxidation reduces considerably the incidence of this ridge around the defects. This is illustrated by comparing the above two 10% HCl 10/20/0/0 and 10% HCl 10/20/0/10 processes to the standard 10/18/2/10 process in the third row. It is believed that the decrease of the ridge in the latter process is a result of the additional 2 min. dry O_2 oxidation following the 18 min. HCl oxidation in the standard process rather than the shorter HCl oxidation (18 min. instead of 20 min.). The influence of HCl concentration and wafer orientation on the structure of the defects in the standard process were well documented in Section 3.1 and 3.2 respectively.

The last two processes studied, the 18/10/2/10 and the 10/10/10/10, were less detrimental to the structure of the oxides. In both processes the $HCl:O_2$ oxidation was ten minutes long and their difference was primarily a redistribution of the dry O_2 oxidation timing. In the 18/10/2/10, most of the 20 min. long dry O_2 oxidation occurred before the HCl oxidation whereas in the 10/10/10/10 process, the 20 min. long dry O_2 oxidation was divided in two 10 min. periods just before and just after the 10 min. HCl oxidation. It can be seen that only the 10% $HCl:O_2$ 18/10/2/10 process on <111> oriented wafers resulted in a visibly non-homogeneous oxide. This suggests that it is not only the duration and the percentage of $HCl:O_2$ that determines the homogeneity of the oxide but also the timing of the HCl oxidation with respect to the dry O_2 oxidation. It is possible that during the post-HCl dry oxidation, some of the chlorine-bearing species diffuse out in the growing oxides.

These last two processes also suggest that the defects in the oxides are not caused by etching of the Si surface by chlorine since the non-homogeneous oxides correspond to the 18/10/2/10 process producing a thicker initial dry O_2 oxide. It can therefore be concluded that the homogeneity of "HCl grown oxides" increases with the duration of the last dry oxidation.

CRC DOCUMENT CONTROL DATA

1. **ORIGINATOR:** Dept. of Communications/Communications Research Centre

2. **DOCUMENT NO:** CRC Report No. 1298

3. **DOCUMENT DATE:** October, 1976

4. **DOCUMENT TITLE:** The Structure of HCl Doped Silicon Oxides and of the Overlaying Metallization

5. **AUTHOR(s):** M. Bouchard, W.A. Hartman and R.M. Kuley

6. **KEYWORDS:**
   (1) Semiconductor
   (2) HCl Oxides
   (3) Semiconductor Metallization

7. **SUBJECT CATEGORY (FIELD & GROUP: COSATI)**

   09 Electronics and Electrical Engineering

   09 01 Components

8. **ABSTRACT:** The addition of chlorine during processing improves the dielectric properties of silicon dioxide by reducing the concentration of mobile ions in the oxide. Since about 1973 the industry has adopted an optimum value of approximately 4 vol % $HCl:O_2$ because of possible detrimental effects at higher concentrations of chlorine. We have found quantitatively that at high concentrations of chlorine (e.g. 10 vol % $HCl:O_2$ mixture) the oxide surface becomes irregular and the excess chlorine forms pockets within the oxide. This work characterizes these oxide defects and shows that their number, size and distribution are influenced by the chlorine concentrations, the processing sequence, the cooling rate following the oxidation, and the wafer orientation. The oxide defects also cause a local lifting of most metallizations and can cause pitting of aluminum. These reliability hazards can be avoided by careful choice of processing parameters.

9. **CITATION:**

BOUCHARD, M.
--The structure of HCI doped silicon oxides and...

TK
5102.5
C673e
#1298

DATE DUE
DATE DE RETOUR

LOWE-MARTIN No. 1137

CRC LIBRARY/BIBLIOTHEQUE CRC
TK5102.5 C673e #1298 c. b
Bouchard, M.

INDUSTRY CANADA / INDUSTRIE CANADA
209143

Government of Canada Gouvernement du Canada